Inverse control and stabilization of free-flying flexible robots
G. de Rivals-Mazères*, W. Yim†, F. Mora-Camino* and S.N. Singh†

SUMMARY
The question of control and stabilization of flexible space robots is considered. Although, this approach is applicable to space robots of other configurations, for simplicity, a flexible planar two-link robot, mounted on a rigid floating platform, is considered. The robotic arm has two revolute joints and its links undergo elastic deformation in the plane of rotation. Based on nonlinear inversion technique, a control law is derived for controlling output variables describing the position and orientation of the platform and the joint angles of the robot. Although, the inverse controller accomplishes reference trajectory tracking, it excites the elastic modes of the arm. For the vibration suppression, three different stabilizer are designed. Using linear quadratic optimal control theory, a composite stabilizer for stabilization of the rigid and flexible modes and a decoupled flexible mode stabilizer are designed for regulating the end point of the robot to the target point and vibration suppression. Stabilization using only elastic mode velocity feedback is also considered. For large maneuvers, first the inverse controller is active, and the stabilizer is switched for regulation when the motion of the robot lies in the neighborhood of the terminal equilibrium state. Simulation results are presented to show that in the closed-loop system including the inverse controller and each of the stabilizers, trajectory tracking and stabilization of elastic modes are accomplished.

KEYWORDS: Flexible manipulator; Free-flying space robot; Vibration stabilization; Position tracking

1. INTRODUCTION
In future space missions, space robots will play important role in the deployment or retrieval of payloads and will be used for the repair and construction of space structures. These robots have long flexible arms. Space robots have complex dynamical behavior. Lack of an inertially-fixed base on which the manipulators are mounted and control-structure interaction pose many difficulties in control system design.

In recent years, researchers have focused attention on the problem of dynamics and control of space robots. Research has been done related to free-flying robots as well to space robots for docking and intercept maneuvers.[1–8] In references 10 and 12 the perturbation technique is used to derive a control law. The control problem is divided into one for the rigid body maneuvering of the robot and one for the feedback control of elastic vibration which is considered as perturbations from the rigid body motion. However, for the suppression of elastic vibrations, one has to find the optimal control law based on an approximate linear time-varying model which is computationally very involved. Controllers have been designed in [7,8,11] for space robots using Lyapunov stability theory. Nonlinear inversion technique has been applied in[13,14] for the space robots, however, control of the spacecraft has not been considered in these. Singular perturbation method has been used to develop continuous path tracking control system for free-flying space robots.[15]

In this paper, a dual mode control system is designed for the control of space robots. Although, this approach is applicable to robots of other configurations, for simplicity, control of a two-link planar robotic arm mounted on a rigid platform, which can translate and rotate about one axis, is considered. The long links of the arm experience transverse deformation in the plane of rotation of the arm. Based on the nonlinear inversion technique, a control system is derived for the trajectory control of the rigid modes (position and orientation of spacecraft and joint angles of manipulator) using the joint torquers and the actuators on the rigid platform. The inverse controller accomplishes reference trajectory tracking, however, it excites the elastic modes of the flexible links. For regulation and vibration suppression to the target equilibrium point, three different stabilizers are designed.

- A linear composite stabilizer for the regulation of rigid and flexible modes
- decoupled flexible mode stabilizer using only actuators located on the links using optimal control theory
- stabilizer using only velocity feedback based on Lyapunov approach

Simulation results are presented which show that in the closed-loop system including the inverse controller and each of the stabilizers, trajectory following and regulation are accomplished. By suitable planning of reference trajectory, desired tasks in space can be performed.

The organization of the paper is as follows. Section 2 presents the problem formulation. An inverse control law is obtained in Section 3. Section 4 presents design of stabilizers, and numerical results are presented in Section 5.

2. MATHEMATICAL MODEL AND CONTROL PROBLEM
Figure 1. shows the space robot mounted on the platform. This configuration of the space robot is similar to that of reference,[7] however, for simplicity, the dynamics of the

* Ecole Nationale de l'Aviation Civile, 7 rue E. Belin, 31055 Toulouse (France)
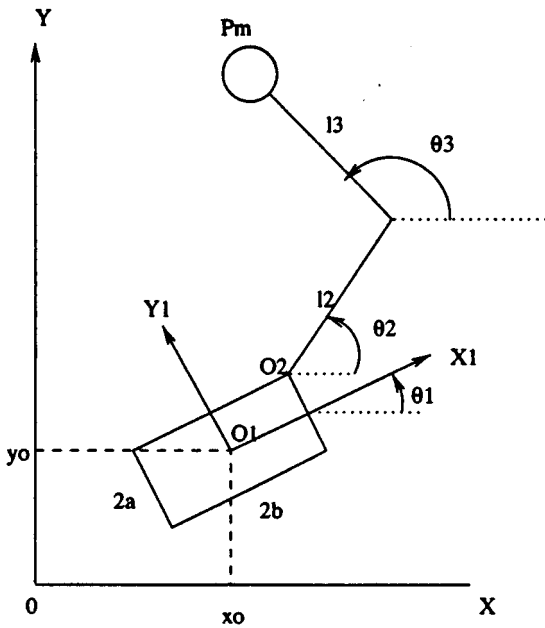† University of Navada Las Vegas, College of Engineering, Las Vegas, NV 89154 (USA)

Fig. 1. Space robot.

wrist have not been included here. The Cartesian coordinates of the platform are denoted as x_0, y_0 and the rotational angle is θ_1 with respect to an inertial frame. The joint angles of the robot are θ_2 and θ_3, measured in the inertial frame. The elastic deformation of the links can be expanded in a series:

$$\delta_i(l_i, t) = \sum_{j=1}^{n_e} \Phi_{ij}(l_i) q_{ij}(t), \quad i = 1, 2$$

where $\Phi_{ij}(l_i)$ are suitable mode shapes, $q_{ij}(t)$ are the generalized coordinates, and l_i is a point on the link i at a distance l_i from the joint.

A complete derivation of equations of motion using Lagrangian approach is given in reference[7]. For the purpose of derivation, one obtains the kinetic and the potential energy. Then, using Lagrange's equations, one obtains the mathematical model given by:

$$M(z)\ddot{z} + h(z, \dot{z}) + Kq = E(\theta)u \quad (1)$$

where the vector of elastic modes is $q = (q_1^T, q_2^T)^T \in \Re^{2n_e}$, $q_i = (q_{i1}, \ldots, q_{in_e})^T \in \Re^{n_e}$, $z = (x_0, y_0, \theta^T, q^T)^T \in \Re^n$, $n = (5 + 2n_e)$, $\theta = (\theta_1, \theta_2, \theta_3)^T$, the control input is $u = (u_r^T, u_f^T)^T$, $u_r = (F_x, F_y, T_1, T_2, T_3)^T \in \Re^5$ and $u_f \in \Re^s$. Here, $M(z)$ is the positive definite symmetric inertia matrix, $h(z, \dot{z})$ represents the Coriolis and centrifugal forces, $K = (0_{5 \times 2n_e}^T, K_1)^T$, K_1 is $(2n_e \times 2n_e)$ positive definite symmetric stiffness matrix, 0 denotes a null matrix of indicated dimensions and E is the control influence matrix. The input u_r consists of the control forces (F_x, F_y) and moment (T_1) acting on the platform and the two joint torques (T_2, T_3) acting on the arm, and u_f denotes the vector of moments applied by actuators located on the flexible links (s is the number of these actuators).

Defining a state vector $x = (z^T, \dot{z}^T)^T \in \Re^{2n}$, the system (1) can be written in a state variable form as:

$$\dot{x} = f(x) + g(x)u \quad (2)$$

where

$$f(x) = \begin{pmatrix} \dot{z} \\ M^{-1}(z)[-h(z, \dot{z}) - Kq] \end{pmatrix}$$

$$g(x) = \begin{pmatrix} 0_{n \times m} \\ M^{-1}(z)E(\theta_1) \end{pmatrix}$$

where $m = 5 + s$.

We associate to system (2) an output vector $y \in \Re^5$ given by:

$$y = (x_0, y_0, \theta^T)^T$$
$$\triangleq C_0 z \quad (3)$$

where $C_0 = (I_5, 0_{5 \times 2n_e})$ and I denotes the identity matrix of indicated dimension.

Suppose that a reference trajectory $y_r(t)$ for $y(t)$ is given. We are interested in deriving a control law such that $y(t)$ tracks $y_r(t)$ and the elastic modes are stabilized. We note that by the appropriate selection of reference trajectories y_r, one can maneuver the platform and the robotic arm to perform variety of tasks.

3. INVERSE CONTROL

In this section, a control law is obtained by the inversion of the input (u_r)-outputs(y) map of the systems (2) and (3) for the trajectory tracking. This choice of input-output map allows independent decoupled control of rigid modes using the joint torquers and the actuators on the platform.

For the inversion of the map, we differentiate y successively till the input appears. Differentiating y and using (2) gives:

$$\dot{y} = C_0 \dot{z}$$
$$\ddot{y} = C_0 M^{-1}(z)[(-h(z, \dot{z}) - Kq) + E_1 u_r + E_2 u_f]$$
$$\triangleq a(x, u_f) + D(z)u_r \quad (4)$$

where $E = (E_1, E_2)$, $a(x, u_f) = C_0 M^{-1}(z)[-h(z, \dot{z}) - Kq + E_2 u_f]$, and $D(z) = C_0 M^{-1}(z)E_1$. Thus the relative degree of $y_i (i = 1, 2)$ is two and the input-output map is invertable since, for the space robot, the 5×5 decoupling matrix $D(z)$ is nonsingular at each z.[16,17]

In view of (4), we choose a decoupling control law of the form:

$$u_r = D^{-1}(z)[-a(x, u_f) + v] \quad (5)$$

where the input v is chosen as:

$$v = \ddot{y}_r - P_2 \dot{\tilde{y}} - P_1 \tilde{y} - P_0 x_s$$
$$\dot{x}_s = \tilde{y} \quad (6)$$

Here, P_i, $i \in \{0, 1, 2\}$ are diagonal matrices and $\tilde{y}$ is the tracking error $y - y_r$. The control signal v is of PID

(proportional, integral and derivative) feedback type. The choice of integral feedback helps in eliminating any constant steady state error in $\tilde{y}$ in the presence of parameter uncertainty.

Substituting control law (5) and (6) in (4) gives:

$$\dddot{y} + P_2\ddot{y} + P_1\tilde{y} + P_0 x_s = 0 \qquad (7)$$

Differentiating (7) once, one obtains a third order linear differential equation for the tracking error given by:

$$\dddot{y} + P_2\ddot{y} + P_1\dot{y} + P_0\tilde{y} = 0 \qquad (8)$$

The matrices P_i are chosen appropriately so that the characteristic polynomial

$$\Pi(\lambda) = det[\lambda^3 I + P_2\lambda^2 + P_1\lambda + P_0]$$

associated with (8) is Hurwitz and thus $\tilde{y}(t) \to 0$ as $\to t \to \infty$ for any initial error $\tilde{y}(0)$. Moreover, if $\tilde{y}(0) = \dot{\tilde{y}}(0) = x_s(0) = 0$, then one obtains from (8) that $y(t) \equiv y_r(t)$, $t \geq 0$ and in the closed-loop system exact tracking of $y_r(t)$ is accomplished.

Although inverse controller is sufficient for the control of the platform and the joint angles of the robotic arm, it causes elastic deformation of the links during maneuver. For point to point control of the end effector, it will be interesting to suppress the vibration of the elastic arm, once the end effector has reached the target point.

4. VIBRATION SUPPRESSION
In this section, stabilization of the elastic modes is considered. Suppose that the chosen reference trajectory $y_r(t)$ converges to y^* (a fixed point) as $t \to \infty$. It is interesting to note that using the inverse controller, one obtains $\tilde{y} \approx 0$ (or $y \approx y^*$) after the initial transient period. As y converges to y^*, only elastic mode oscillations persist in the closed-loop system including the inverse controller. Thus, in the terminal phase, the motion of the space robot lies in the vicinity of the equilibrium point $x^{*T} = (z^{*T}, \dot{z}^{*T} = 0)$ where $z^{*T} = (y^{*T}, q^{*T} = 0)$, and therefore, the system can be well approximated by a linear system in the neighborhood of x^*.

For the regulation to the terminal state, we shall consider three kinds of stabilizers in this section.

4.1 Inverse control, and rigid and elastic mode stabilizer
For the design of a stabilizer, we linearize the system about the equilibrium point x^*. Neglecting the second order terms in velocity $\dot{z}$, one obtains the linearized system from (1) of the form:

$$M(z^*)\Delta\ddot{z} + Kq = E(\theta_1^*)u \qquad (9)$$

where $\Delta z = z - z^*$, $\Delta\dot{z} = \dot{z}$, and $\Delta\ddot{z} = \ddot{z}$. In view of (1), at the equilibrium point x^*, one has $u = u^* = 0$.

Defining $\tilde{x} = (\Delta(z)^T, \Delta(\dot{z})^T)^T$, one obtains the linearized system:

$$\dot{\tilde{x}} = A\tilde{x} + Bu \qquad (10)$$

where

$$A = \begin{pmatrix} 0_{n \times n} & I_{n \times n} \\ A_{21}(z^*) & 0_{n \times n} \end{pmatrix} B = \begin{pmatrix} 0_{n \times m} \\ M^{-1}(z^*)E(\theta_1^*) \end{pmatrix},$$

$$A_{21}(z^*) = (0_{n \times 5}, -M^{-1}(z^*)K)$$

For stabilization of the system (10), one uses the linear quadratic optimal control technique. We choose a performance index of the form:

$$J = \int_0^\infty (\tilde{x}^T Q\tilde{x} + u^T Ru)dt \qquad (11)$$

By a suitable choice of the positive definite symmetric weighting matrices Q and R, and by minimizing J, one obtains the optimal control input:

$$u = -R^{-1}B^T S\tilde{x} \triangleq -F\tilde{x} \qquad (12)$$

where S is the solution of the Riccati equation.[18]

For the maneuver of the space robot, the controller is implemented as follows: First, the inverse control u_r is made active for large translational and rotational maneuvers of the space robot. When the output vector $y(t)$ reaches the vicinity of y^*, the inverse controller is switched off and the elastic mode stabilizer is switched on. Thus, in the terminal phase, only the elastic mode stabilizer is active and the terminal regulation of the state x to the equilibrium point x^* is accomplished by the linear feedback law (12).

The closed-loop system is shown in Figure 2.

4.2 Inverse control, and decoupled flexible mode stabilization
Now we consider decoupled rigid mode control and flexible mode stabilization using only elastic link actuators. Since the inverse controller accomplishes steering of y to y^*, setting $\dot{y} = 0$, $\ddot{y}$ in (9) gives:

$$M_{12}(z^*)\ddot{q} = E_{11}(\theta_1^*)u_r + E_{12}u_f \qquad (13)$$

$$M_{22}(z^*)\ddot{q} + K_1q = E_{21}u_r + E_{22}u_f \qquad (14)$$

Substituting the value of u_r from (13) into (14) gives:

$$[M_{22}(z^*) - E_{21}E_{11}^{-1}M_{12}(z^*)]\ddot{q} + K_1q =$$
$$(E_{22} - E_{21}E_{11}^{-1}E_{12})u_f \qquad (15)$$

Defining $x_f = (q^T, \dot{q}^T)^T$, a state variable representation of (15) is:

$$\dot{x}_f = A_f x_f + B_f u_f \qquad (16)$$

where

$$\hat{M}_{22} = (M_{22} - E_{21}E_{11}^{-1}M_{12})$$

$$E_f = (E_{22} - E_{21}E_{11}^{-1}E_{12})$$

$$A_f = \begin{pmatrix} 0_{2n_e \times 2n_e} & I_{2n_e \times 2n_e} \\ -\hat{M}_{22}^{-1}K_1 & 0_{2n_e \times 2n_e} \end{pmatrix}$$

$$B_f = \begin{pmatrix} 0_{2n_e \times 2n_e} \\ \hat{M}_{22}^{-1}E_f \end{pmatrix}$$

Remark 1: Although the design approach has been applied to a simple robot of two links, it should be pointed out that inverse controller design approach is equally applicable to robots of n_l links mounted on a space vehicle experiencing
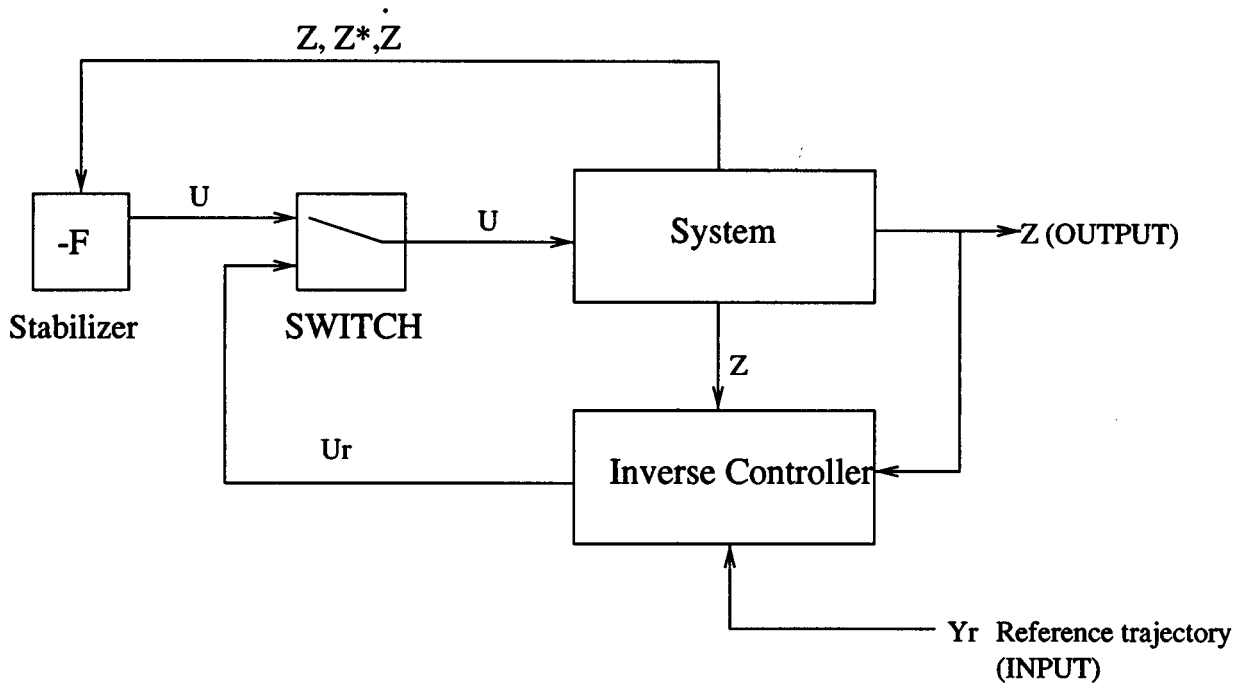
Fig. 2. Closed-loop control system.

three dimensional motion with six actuators. Thus each of the rigid modes can be independently controlled using a similarly designed inverse controller with $(6+n_l)$ actuators.

4.2.1 Optimal decoupled stabilization. For obtaining an optimal stabilizer we choose the performance index

$$J_f = \int_0^\infty (x_f^T Q_f x_f + u_f^T R_f u_f) dt \qquad (17)$$

where Q_f and R_f are positive definite. The optimal control is obtained using minimized linear quadratic optimization technique. It is of the form:

$$u_f = -R_f^{-1} B_f S_f x_f \triangleq -F_f \times [q^T, \dot{q}^T]^T \qquad (18)$$

where S_f is the solution of the Riccati equation.

Remark 2: For the space vehicle with n_l links robot, one obtains a higher order of equations describing the flexible modes of each link. Since (n_l+6) rigid modes are decoupled, stabilizing control law is derived which is similar to (18).

4.2.2 Decoupled stabilization using a velocity feedback. It is interesting to examine stabilization of the flexible modes using only the velocity feedback. For the design of stabilizer, we neglect the matrix E_{21} in (14) since it is small. We choose the stabilization signal of the form:

$$u_f = -\lambda E_{22}^T \dot{q} \qquad (19)$$

where $\lambda > 0$. For proving stability of the system (14) and (19) with $E_{21}=0$, we use the Lyapunov stability theory. We choose a positive definite function:

$$W(x_f) = \dot{q}^T M_{22}(z^*)\dot{q} + q^T K_1 q \qquad (20)$$

Then the derivative of W along the solution of the system (14) and (19) is given by:

$$\dot{W}(x_f) = -2\lambda \dot{q}^T E_{22} E_{22}^T \dot{q} = -2\lambda \parallel E_{22}^T \dot{q} \parallel^2 \leq 0$$

Thus, $\dot{W} \equiv 0$ if $E_{22}^T \dot{q} \equiv 0$. It easily follows that if the matrix pair (C_f, A_f) is observable where $C_f = (0, E_{22})$, then the largest invariant set contained in the set $\Omega = \{x_f \in \Re^{4n_e} : \dot{q} = 0\} = \{0\}$ and the origin $x_f = 0$ of the system (16) and (19) is asymptotically stable.[19]

In this section we have obtained three stabilizers (12), (18), and (19). Using stabilizer (12), one obtains efficient stabilization of the rigid as well as flexible modes since all the actuators are used for regulation. However, computation of gain matrix F is relatively complex due to the high order of the system. Unlike stabilizer (12), only actuators on the flexible links are used for stabilization of the flexible modes. The inverse controller independently accomplishes reference trajectory tracking. Although the stabilizer (18) or (19) are switched on in the vicinity of the terminal state, it does not affect the tracking ability of the inverse controller. The stabilizer (19) uses only the velocity feedback and it does not need the computation of the Riccati equation.

5. SIMULATION RESULTS
In this section, numerical results are presented. The complete closed-loop system (1) with the inverse controller (5), and the stabilizer (11) or (12) is simulated. The parameters of the space robot are:

$a = 0.5m, b = 0.5m$

$l_2 = 1m, l_3 = 1m$

$m_{platform} = 10kg, m_{l_2} = 1kg, m_{l_3} = 1kg, pm = 200g$

$EI = 120N/m^2$

The feedback gains are chosen as $P_2 = 3\lambda_e I_{5\times 5}$, $P_1 = 3\lambda_e^2 I_{5\times 5}$, and $P_0 = \lambda_e^3 I_{5\times 5}$. With these choices of P_i, the characteristics roots of (8) are at $\lambda = -\lambda_e$. For the simulation, λ_e was equal to 1. Taking the notations of Section 2, we have $n_e = 2$, $n = 9$, $s = 4$: this means we have considered two of the elastic modes of each half-arm and we have added four actuators.

The initial and final conditions are as follows:
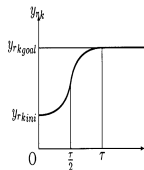
	Initial	Final
x_0 (m)	5	0
y_0 (m)	-10	0
θ_1 (°)	60	90
θ_2 (°)	45	90
θ_3 (°)	90	0
Elastic deflection	null	null

We have chosen $\dot{z}(0) = 0$.

Each component y_{r_k} of the command trajectory was computed as a "S" curve using the initial and final values of y and the following equations (here $\tau = 5s$):

$$t \in \left[0; \frac{\tau}{2}\right] \quad y_{r_k} = y_{r_{kini}} + \frac{y_{r_{kgoal}} - y_{r_{kini}}}{2} \frac{4}{\tau^2} t^2$$

$$t \in \left[\frac{\tau}{2}; \tau\right] \quad y_{r_k} = y_{r_{kgoal}} - \frac{y_{r_{kgoal}} - y_{r_{kini}}}{2} \frac{4}{\tau^2} (t - \tau)^2$$

$$t \in \left[\tau, +\infty\right] \quad y_{r_k} = y_{r_{kgoal}}$$

5.1 Trajectory control: $u_f = 0$
The closed-loop system (1) and (5) was simulated without the stabilizer. Selected responses are shown in Figure 3. In this case, perfect tracking of y_r is accomplished ($y \equiv y_r$), however persistent bounded elastic mode oscillation exists.

5.2 Tracking, and rigid and elastic mode stabilization
The complete closed-loop system (1), (5) and (12) was simulated. The optimal stabilizer was designed using the
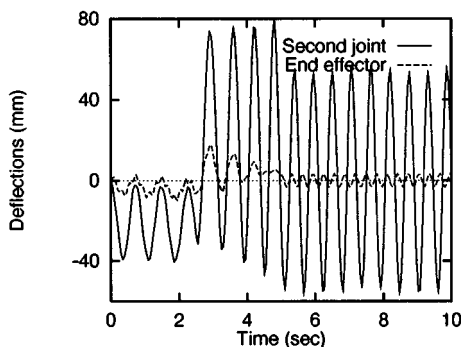
weighting matrices Q and R selected as:

$$Q = diag[1; 1; 1; 1; 1; 0.8; 0.8; 0.8; 0.8;$$
$$0.3; 0.3; 0.3; 0.3; 0.3; 0.2; 0.2; 0.2; 0.2]$$

and $R = I_{9\times 9}$.

The eigenvalues of the closed-loop system matrix $A_c = (A - BF)$ are:

$$\begin{cases} -0.200776 \pm 0.198379_j \\ -0.203102 + 0.200635_j \\ -0.487423 + 0.455377_j \\ -1.09089 \pm 0.820105_j \\ -1.8525 \pm 0.882634_j \\ -12.8329 \pm 83.6529_j \\ -8.92213 \pm 98.3441_j \\ -189.774 \pm 423.539_j \\ -146.679 \pm 455.667_j \end{cases}$$

Initially, only the inverse controller is active and stabilizer is switched at $t = 5s$. Figure 4(a) shows the evolution of the coordinates of the platform, its orientation, and the evolution of the angles of the joints of the robot. Switching of stabilizer after 5 seconds causes only a small tracking error (the maximum tracking error is $(y - y_r)_{max} = (10mm, 0.6mm, 0.7°, 0.9°, 0.1°)^T$). The control magnitudes are reasonable (see Figure 4(b)). We observe smooth regulation of the space robot to the terminal state: the deflections of the end point of each link are shown in Figure 4(c). Of course, there exist enough flexibility in the control system, and the parameters P_i, Q, R command trajectory, and the switching instant are properly chosen to obtain desirable responses.

Fig. 3. Inverse Controller alone: deflections at the end of each half-arm.
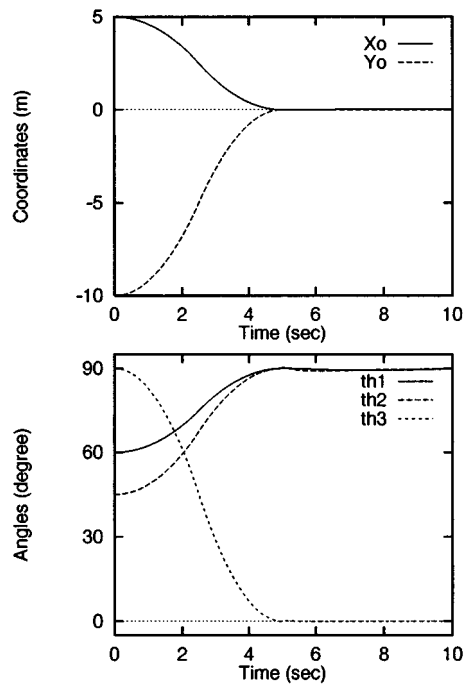

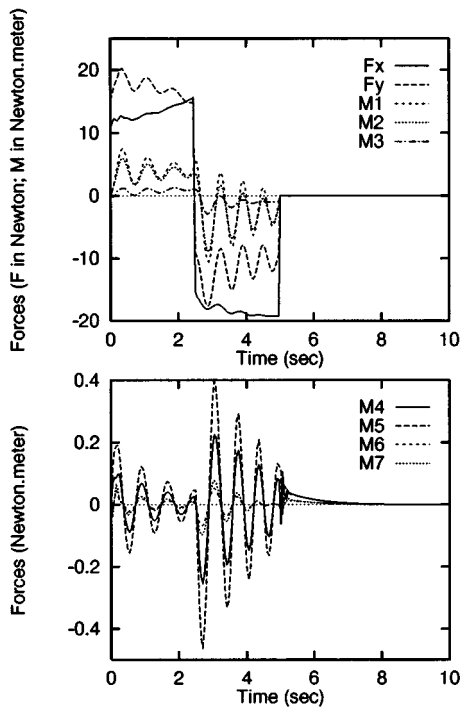Fig. 4a. Coordinates and Orientation of the platform; angles of the joints.

Fig. 4b. Value of the actuators.

One can reduce control magnitude by choosing slower command trajectory. The evolution of the trajectory of the robot is shown in Figure 4(d).

To examine the capability of the stabilizer, the system (1) and (12) was simulated, but inverse controller (5) was not used: optimal stabilizer was switched on from the beginning. Here, there is no reference trajectory: the controller aims at minimizing $z - z^*$ and $\dot{z}$ without any other goal. The state vector does converge to the terminal point but very slowly ($40s$ instead of $5s$ previously): see Figure 5(a). On the other hand, the deflections are small (see Figure 5(b)). This simulation shows that the robot may be controlled with the optimal stabilizer alone even if the initial state is quite far from the terminal point.

5.3 Inverse control and decoupled elastic mode stabilization

Simulation was done using the closed-loop system (1), (5) and the stabilizers of section 4.2 (stabilization of the flexible modes only: 4 actuators are used instead of 9 in the previous section).
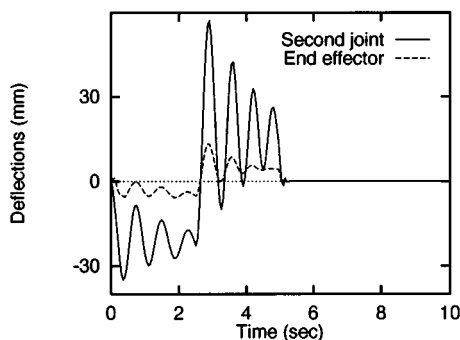

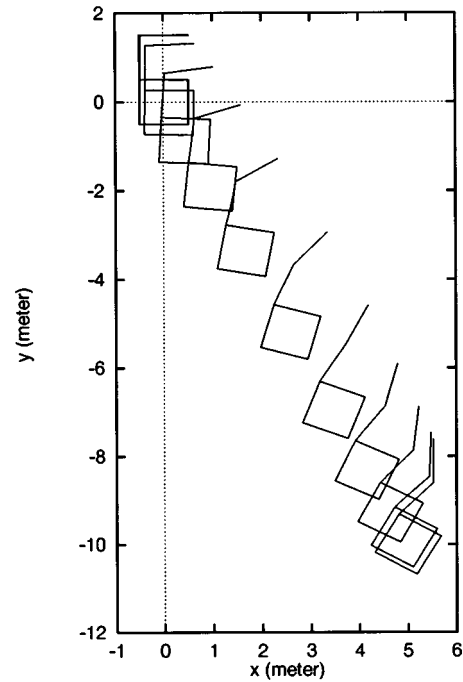Fig. 4c. Deflections at the end of each half-arm.

Fig. 4d. Evolution of the robot.

5.3.1 Optimal decoupled stabilization. An optimal stabilizer (18) was designed using the weighting matrices as:

$$Q = diag[1; 1; .8; .8; .3; .3; .2; .2] \text{ and } R = I_{4 \times 4}$$

The eigenvalues of the closed-loop system matrix $A_{cf} = (A_f - B_f F_f)$ are:

$$\begin{cases} -0.645224 \pm 11.1454_j \\ -0.76032 \pm 20.2767_j \\ -3.79561 \pm 124.082_j \\ -4.07113 \pm 141.854_j \end{cases}$$
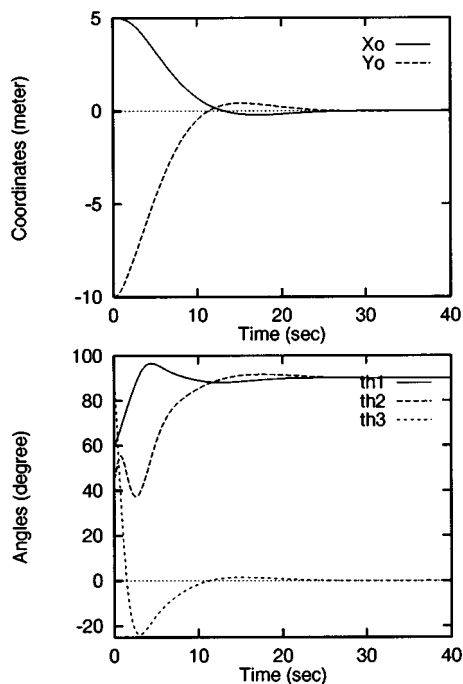

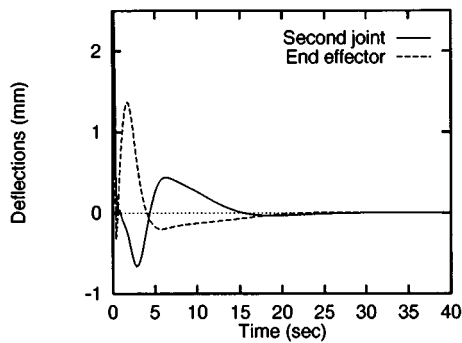Fig. 5a. Coordinates and Orientation of the platform; angles of the joints.

Fig. 5b. Deflections at the end of each half-arm.

Stabilizer was switched on at $t=5s$. Selected responses are shown in Figure 6. We observe smooth stabilization of the elastic modes. Unlike Figure 4(a), perfect tracking is accomplished in this case ($\tilde{y} \equiv 0$).

5.3.2 Decoupled stabilization using velocity feedback. The closed-loop system (1), (5) and stabilizer (19) with $\lambda=1$ was simulated. This stabilizer uses only the elastic mode velocity $\dot{q}$ feedback. Selected responses are shown in Figure 7. Interestingly, smooth suppression is accomplished only by velocity feedback. As predicted, the tracking error is null: $y - y_r \equiv 0$ because u_f and u_r are independent. Here, 5
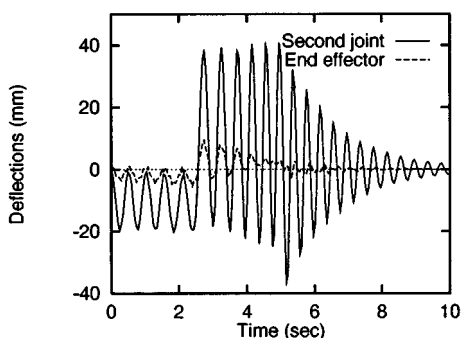

Fig. 6. Inverse Control and stabilization of flexible modes with the 4-actuator optimal stabilizer switched on at $t=5s$: deflections at the end of each half-arm.
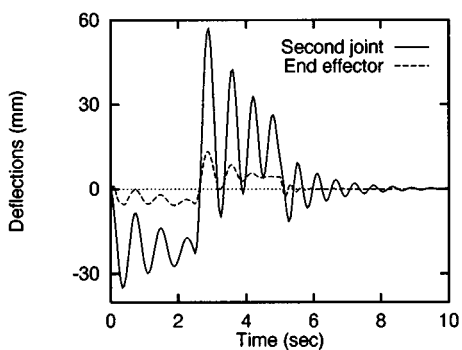

Fig. 7. Inverse Control and Velocity feedback stabilizer: deflections at the end of each half-arm.

actuators accomplish tracking of the reference trajectory and the 4 actuators located on the flexible links suppress the vibration.

6. CONCLUSION

A design approach for the control of space robots based on nonlinear inversion technique and optimal control theory was presented. Space vehicle actuators and the joint torquers were used for reference trajectory tracking of rigid modes. Although, the inverse controller accomplishes trajectory control, it excites the elastic modes of the arm. For vibration suppression and regulation to the terminal state, three different kinds of stabilizers were designed using linear quadratic optimal control theory and velocity feedback. The first stabilizer was designed using a linearized complete model for the stabilization of the rigid and flexible modes. The decoupled flexible dynamics were used to design the second stabilizing control law using only the actuators located on the links. These two stabilizers were designed using optimal control theory. The third stabilizer was designed for decoupled elastic mode stabilization using only elastic mode velocity feedback. Simulation results showed that in the closed-loop system precise tracking and regulation are accomplished using the inverse controller and the stabilizers.

References
1. R.W. Longman, "The kinetics and workspace of a satellite-mounted robot", *J. Astronautical Sciences* **38**, No. 4, 423–439 (1990).
2. R.E. Lindberg, R.W. Longman and M.F. Zedd, "Kinetic and dynamics properties of an elbow manipulator mounted on a satellite", *J. Astronautical Sciences* **38**, No. 4, 397–421 (1990).
3. Z. Vafa and S. Dubowsky, "On the dynamics of space manipulators using the virtual manipulator, with applications to path planning" *J. Astronautical Sciences*, **38**, No. 4, 441–472 (1990).
4. H.L. Alexander, and R.H. Cannon, "An extended operational-space control algorithm for satellite manipulators", *J. Astronautical Sciences* **38**, No. 4, 473–486 (1990).
5. D. Nenchev, Y. Umetani, and K. Yoshida, "Analysis of a redundant free-flying space-craf/manipulator system", *IEEE Transactions on Robotics and Automation* **8**, No. 1, 1–6 (1992).
6. Y. Nakamura and R. Mukherjee, "Nonholonomic path planning via a bidirectional approach", *IEEE Transactions on Robotics and Automation* **7**, No. 4, 500–514 (1991).
7. L. Meirovitch and L. Seungchul, "Maneuvering and control of flexible space robots", *J. Guidance, Control, and Dynamics* **7**, No. 3, 520–528 (1994).
8. Y. Chen and L. Meirovitch, "Control of a flexible space robot executing a docking maneuver", *J. Guidance, Control, and Dynamics* **18**, No. 4, 756–766 (1995).
9. L. Meirovitch and R.D. Quinn, "Equations of motion for maneuvering flexible space-crafts", *J. Guidance, Control, and Dynamics* **10**, No. 5, 453–465 (1987).
10. L. Meirovitch and M.K. Kwak, "Control of flexible spacecraft with time-varying configuration", *J. Guidance, Control, and Dynamics* **15**, No. 2, 314–324 (1992).
11. V.J. Modi and J.K. Chang, "Performance of an orbiting flexible mobile manipulator", *Transactions of the ASME: Journal of Mechanical Design* **113**, 516–524 (1991).

12. L. Meirovitch and Y. Chen, "Trajectory and control optimization for flexible space robots" *J. Guidance, Control, and Dynamics* **18**, No. 3, 493—502 (1995).
13. S.N. Singh and A.A. Schy, "Control of elastic robotic systems by nonlinear inversion and modal damping", *J. Dynamic Systems, Measurement and Control* **108**, 180–189 (Sept., 1986).
14. S.N. Singh and A.A. Schy, "Elastic robot control: Nonlinear inversion and Linear stabilization", *IEEE Transactions on Aerospace and Electronic Systems* **AES-22**, No. 4, 340–348 (July, 1986).
15. Y. Murotsu, K. Senda, A. Mitsuya and K. Yamane, "Theoretical and experimental studies for continuous path control of flexible manipulator mounted on a free-flying space robot"", *AIAA Guidance, Navigation and Control Conference*, Montevery, C.A. (August, 1993) pp. 1458–1471.
16. S.N. Singh and W.J. Rugh, "Decoupling in a class of nonlinear systems by state variable feedback", *J. Dynamic Systems, Measurement and Control* **94**, 323–329 (1972).
17. A. Isidori, *Nonlinear Control Systems* (Springer-Verlag, New York, 1985).
18. M. Athans and P.L. Falb, *Optimal Control: An Introduction to The Theory and its Applications* (McGraw-Hill, New York, 1966).
19. M. Vidyasagar, *Nonlinear Systems Analysis* (Prentice Hall, Englewood Cliffs, New Jersey, 1978).